Journal of Molecular Catalysis A: Chemical 404 (2015) 65–73

Contents lists available at ScienceDirect

Journal of Molecular Catalysis A: Chemical

journal homepage: www.elsevier.com/locate/molcata

Biomass toward fine chemical products: Oxidation of α-pinene over sieves nanostructured modified with vanadium

Analía L. Cánepa[a], Corina M. Chanquía[b], Virginia M. Vaschetti[a], Griselda A. Eimer[a], Sandra G. Casuscelli[a,*]

[a] Centro de Investigación y Tecnología Química (CITeQ), UTN-CONICET, Facultad Regional Córdoba, Maestro López esq. Cruz Roja Argentina, S/N, X5016ZAA, Córdoba, Argentina
[b] Centro Atómico Bariloche, Comisión Nacional de Energía Atómica, CNEA-CONICET, Bustillo 9500, S.C. de Bariloche, R8402AGP, Río Negro, Argentina

ARTICLE INFO

Article history:
Received 20 January 2015
Received in revised form 6 April 2015
Accepted 13 April 2015
Available online 15 April 2015

ABSTRACT

Vanadium-containing molecular sieves (V-M(*x*)) were synthetized and applied as heterogeneous catalysts for the liquid phase oxidation of α-pinene with hydrogen peroxide at 70 °C. It has been found that the vanadium content in V-M(*x*) materials affected the conversion of α-pinene and product distribution. The turnover numbers increased strongly with the decreasing of V content probably caused by a high V dispersion. The major products were verbenone, *trans*-sobrerol and campholenic aldehyde. The acid–base properties of V-M(*x*) affected the distribution of products formed via the isomerization of α-pinene oxide over Lewis acid sites to campholenic aldehyde while Brønsted acid sites brought about the formation of 1,2 pinanediol and *trans*-sobrerol by hydrolysis and by the opening of oxirane ring. The increase in V content in V-M(*x*) led to the increase in campholenic aldehyde, 1,2 pinanediol, *trans*- sobrerol and over oxidation products. Moreover, the effect of several solvents on the reaction oxidation was studied. The results showed that the highest α-pinene conversions are obtained in the following order: acetonitrile > ethanol > isoamyl alcohol > methyl ethyl ketone. Thus, using aprotic solvents, the catalytic activity was increased and the formation of alkyl glycol ethers as by-product was not observed.

The catalysts were characterized by ICP-OES, N_2 adsorption, UV-Vis-DR, FT-IR, Raman and FT-IR with pyridine adsorption. The results confirmed that the V-M(*x*) samples possessed regular and stable structure with a high specific surface. The V atoms were successfully introduced mainly as tetrahedral coordinated isolated species into the MCM-41 framework, which would be located either inside the wall or on the surface of the mesoporous cannel.

Leaching experiments demonstrated that very small amounts of V species were leached from the solid matrix only during the first and second catalytic cycle as not active species. Acetonitrile and H_2O_2 were involved in the lixiviation reaction forming inactive soluble V species, while the isolated $V^{\delta+}$ cations were stable active sites for the oxidation of α-pinene. In addition, the catalyst also showed stability in its structure. Finally, the recycling experiments showed that the most active catalyst can be used repeatedly without activity and selectivity loss during several cycles.

1. Introduction

In recent years, considerable attention has been focused on the development of environmentally sustainable processes, in particular the synthesis of chemical compounds from biomass. Thus, terpenic compounds, abundant in nature, are an important renewable feedstock for the flavor and fragrance industry. The oxyfunctionalization of monoterpenes represents an interesting route to extend the utilization of these cheap natural products. Their oxygenated derivatives usually show interesting organoleptic properties and form one of the most important groups of fragrance ingredients [1]. These compounds are also commercially important materials for pharmaceutical industry as well as useful synthetic intermediates and chiral building blocks [2]. Among terpenes, α-pinene is an abundant and suitable feedstock for the production of verbenone. This is product of the allylic oxidation of α-pinene and it is widely used for the synthesis of taxol, an important therapeutic agent. In the area of liquid-phase oxidations, the use of nanocatalysts such as transition metals-modified M41S type molecular sieves emerged as an interesting option for the development of environmental compatible processes, especially in the fine chemical synthesis, substituting the homogeneous catalysis.

* Corresponding author at: CITeQ-UTN-CONICET, Facultad Regional Córdoba, Argentina. Tel.: +54 351 4690585; fax: +54 351 4690585.
E-mail address: scasuscelli@scdt.frc.utn.edu.ar (S.G. Casuscelli).

http://dx.doi.org/10.1016/j.molcata.2015.04.009
1381-1169/

MCM-41, a typical mesoporous molecular sieve, possesses a large surface area as well as well-ordered channels with controllable uniform pore size of 2–10 nm, which allows a faster diffusion of large organic molecules than smaller channel microporous molecular sieves [3]. Interestingly, other atoms different from silicon can be incorporated into the mesoporous silica matrix, giving the final material catalytic properties. This is the case of V-substituted mesoporous molecular sieves V-MCM-41, which can be prepared by several synthesis procedures [4–8]. However, there is considerable debate over the stability of metal- containing mesoporous materials, and in a more generalized way, it is argued that the isomorphously substituted metal species on the silicate framework would not leach easily under reaction conditions and hence, they exist as true heterogeneous catalysts. V-containing mesoporous molecular sieves were found to be active in a number of liquid phase oxidation reactions using H_2O_2 as an oxidant [8–11]. The activity and selectivity of these catalysts were found to be sensitive to the nature of V species in the matrix, which includes oxidation state, coordination condition, dispersion and stability [12]. Besides dispersing and stabilizing V species, the structural features of macroporous supports also have effects on the form of V species and their catalytic behavior. Thus, Luan et al. [3] synthesized and characterized V-MCM-41 and they concluded from their studies that V occurs simultaneously in two forms on the support surfaces, as framework and extra-framework species. Moreover, the presence of isolated metal species is an important factor for efficient catalytic oxidation using peroxides as oxidants, since the presence of metallic oligomers causes a fast decomposition of the peroxide [13].

On the other hand, the synthesis of fine chemical over solid catalysts often involves the use of solvents that may strongly influence the activity and selectivity. Thus, the properties of solvents and their impact on processes lies at the heart of process development in many industry sectors particularly pharmaceuticals, agrochemicals and fine chemical. The choice of suitable solvents is frequently critical to obtain high catalytic activity and selectivity. However, the optimal solvent selection needs a more detailed knowledge on the relationship between the chemical nature of the solvent and the interactions taking place in the liquid–solid catalytic systems in fine chemical synthesis.

Furthermore, the stability and heterogeneity are two important factors that determine the applicability and reusability of any mesoporous material in liquid phase oxidation reactions. In this context, it is the aim of this work to investigate influence of the V content and the nature of the solvent on the catalytic activity and selectivity of V-M(x) for the oxidation of α-pinene using H_2O_2 as oxidant. Thus, we have selected four solvents having different polarities (dielectric constants). Moreover, the influence of the protic/aprotic nature of the solvent has also been studied. These solvents were also chosen because they form a single phase with the α-pinene and the H_2O_2, so mass transfer problems associated with the presence of different liquid phases were avoided. In addition, the nature of V species formed on mesoporous molecular sieves under study and their structural properties were analyzed. The stability and heterogeneity of the synthetized materials were further verified in the oxidation reaction of α-pinene through a series of heterogeneity studies.

2. Experimental

2.1. Catalyst synthesis and characterization techniques

The metal- free MCM-41 mesoporous molecular sieve (Si-MMS) was synthesized as previously reported [14]. The V-containing mesoporous molecular sieves were prepared using Tetraethoxysilane (TEOS, Fluka > 98 %) as a source of Si, $VO(SO_4)$. H_2O (Aldrich, 99,99 %) as V source and ethanol solution of cetyltrimethyl ammonium bromide (CTABr, Aldrich) which was used as template, as described in [11]. Mole compositions of the starting gel of the material used in this study were: Si/V = 20, 60 and 240, OH/Si = 0.3, template/Si = 0.3, H_2O/Si = 60. The template was evacuated from the samples by heating (2 °C/min) under N_2 flow (45 mL/min) at 500 °C for 6 h and subsequent calcination at 500 °C for 6 h under dry air flow (45 mL/min). These V-modified catalysts were named as V-M(x), where x indicates the Si/V molar ratio in the synthesis gel. The characterizations of the materials evaluated in this work were previously reported [11]. Here, we mention only those aspects which are relevant to the catalytic activity. Raman spectra were taken on a LabRamHR Horiba Raman spectrometer using 514 nm laser. Infrared analysis of the samples was recorded on a JASCO 5300 FT-IR spectrometer. The FT-IR spectra in the lattice vibration region were performed using the KBr 0.05% wafer technique. In addition, the fresh and used catalyst in the oxidation reaction were analyzed by diffuse reflectance UV–Vis spectroscopy (UV-Vis-DR Jasco V 650), Inductively coupled plasma optical emission spectroscopy (VISTA-MPXCCD Simultaneos ICP-OES – VARIAN) and N_2 adsorption/desorption isotherms (Micromeritics ASAP 2010).

2.2. Oxidation of α-pinene

In a typical reaction, α-pinene ($C_{10}H_{16}$, Fluka > 95 %) (7.17 mmol), hydrogen peroxide (H_2O_2, Riedel de Haën, 35 wt.% in water) (1.79 mmol), acetonitrile (AcN, Sintorgan, 99.5 %) (107.56 mmol) as solvent and V-M(x) (63 mg) were placed in a pirex glass reactor. This reactor, equipped with a condenser to reflux and magnetically stirred, was immersed in a thermally controlled bath at 70 °C. Reaction progress was followed taking samples at different times by a lateral tabulation, without opening the reactor. Liquid samples were immediately filtered and analyzed by gas chromatography using a capillary column crosslinked methyl-silicone gum, 30 m × 0.53 mm × 2.65 mm film thickness and connected to a FID detector. The percentage of each component in the reaction mixture was calculated by using the method of area normalization employing response factors. The α-pinene conversion was defined as the ratio of converted species to initial concentration and the selectivity as (mol product/mol total products) × 100. The turnover number (TON) was defined as moles of olefin converted/mol of metal in the catalyst. Finally, the total conversion of H_2O_2 was measured by iodometric titration and the H_2O_2 efficiency was calculated as the percentage of this reactive converted to total oxidized products. The used catalyst was collected and regenerated by calcination at 500 °C for stability and heterogeneity tests.

3. Results and discussion

3.1. Catalyst characterization

Table 1 shows the chemical composition and textural properties of V-M(x) material used in this study. As it can be observed, all of the samples showed a specific surface higher than 900 m^2/g, which is typical of mesoporous materials. Nevertheless, this parameter was slightly decreased with the metal content. Diffuse-reflectance UV–Vis spectra are useful and reliable in the detection of the presence of framework and extraframework metal species in metal-containing mesoporous materials. The UV-Vis-DR spectra of V-M(x) samples, previously dehydrated in air at 500 °C during 12 h, are given in Fig. 1 and the relative proportions of the deconvoluted peaks are showed in Table 1. The deconvolution of bands reveals three main absorption features at 250, 290 y 320 nm corresponding to: isolated V ions tetrahedral coordinated with oxygen ligands

Table 1
Chemical composition, specific surface and vanadium species relative distribution in V-M(*x*).

Sample	Si/V[a]	V content[b](wt.%)	A_{BET}[c](m^2/g)	Distribution of V-nanospecies[d] (area%)			
				$V^{\delta+}$ inside wall	$V^{\delta+}$on wall surface	$V^{\delta+}$in extraframework clusters	
				~250 nm	~290 nm	~320 nm	~380 nm
V-M(20)	20	1.210	934	54	19	11	16
V-M(60)	60	0.140	1380	62	23	15	–
V-M(240)	240	0.035	1370	71	15	13	–
Si-MMS	∝	0.000	1520	–	–	–	–

[a] Molar ratio in the initial synthesis gel.
[b] In the final solid.
[c] BET specific surface area.
[d] From UV-Vis-RD data.

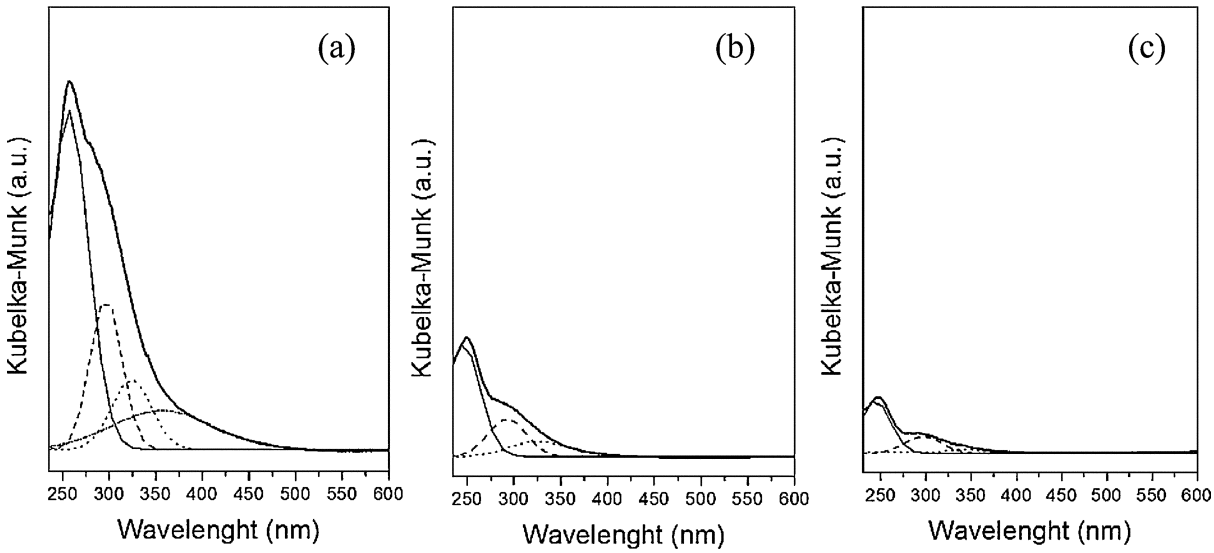

Fig. 1. Diffuse reflectance UV-Vis spectra of calcined samples where: (a) V-M(20), (b) V-M(60), (c) V-M(240).

inside the walls, on the wall surfaces [3,15] and V corresponding to higher coordinated $V^{\delta+}$ ions in an octahedral environment [15,16] respectively. From results shown in Table 1, the distribution of these V species depends on the quantity of V in the initial gel. Thus, the most of the V is incorporated into the structure as tetrahedral coordinated isolated V species. On the other hand, the increase of V content would be causing an increase in the degree of polymerization of the V species giving rise to the formation of the $(V^{\delta+}\cdots O^{\delta-}\cdots V^{\delta+})_n$ nanoclusters arising from an incipient oligomerization of V species [16–18]. These species would be increasing its size when the V content increases, judging by the appearance of an absorption band at higher wavelength (380 nm) for the V-M(20) sample.

Raman spectroscopy was employed in late complement the information already obtained by UV-Vis-RD. Fig. 2 shows the Raman spectra of calcined V-M(*x*) samples and the pure siliceous Si-MMS. The introduction of vanadium species in the MCM-41 structure gives Raman bands at 269, 335, 920 and 1018 cm^{-1}. Thus, the Raman band of 1018 cm^{-1} corresponds to the stretching frequency of a terminal of V=O group bonded to the silicate MCM-41 [9,12]. In addition, the Raman band at 269 cm^{-1}.

FT-IR spectra of Si-MMS and V-M(*x*) samples are shown in the Fig. 3. The main bands described in the literature for MCM-41 are found in our samples, particularly the bands at around 1089 and 1243 cm^{-1} associated to asymmetric Si—O stretching modes, as well as the bands at 800 and 458 cm^{-1} assigned to symmetric stretching and tetrahedral bending of Si—O bonds, respectively [19,20]. However, the band associated with stretching frequency of framework Si—O—Si bonds shifts from 1089 cm^{-1} (Si-MMS (d)) to 1082 cm^{-1} (V-M(*x*), curves (a)–(c)). Then, this may support the

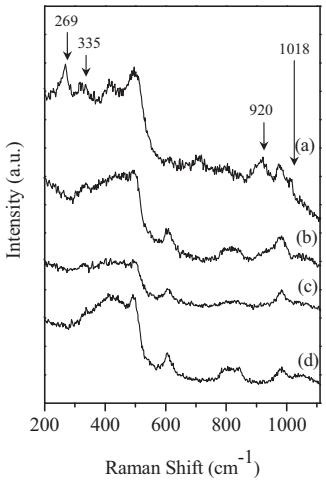

Fig. 2. Raman spectra of (a) V-M(20), (b) V-M(60), (c) V-M(240) and (d) Si-MMS

incorporation of vanadium into MCM-4 framework [3]. Moreover, a strong band at 960 cm^{-1} is clearly visible in all of the spectra. Several authors have assigned this band to the incorporation of heteroatoms such as Ti or V into the framework of the mesoporous silica materials [7,9,21]. Thus, Wu, et al. [8] attributed the presence of bands at 960 cm^{-1} to the framework V—O—Si stretching vibrations. However, caution is required in assigning this band since pure silica MCM-41 also exhibits such band around 960 cm^{-1} attributed to the Si—O stretching vibration in the Si—O—H groups of the silica

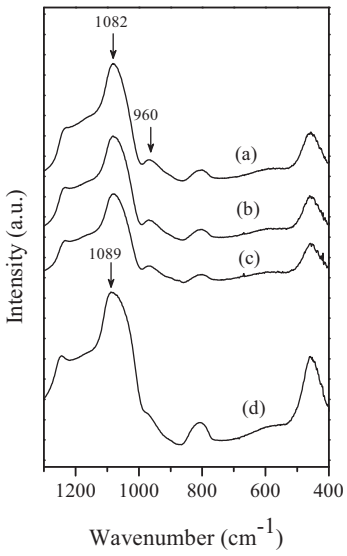

Fig. 3. FTIR absorption spectra in the 400–1300 cm^{-1} range of calcined samples where: (a) V-M(20), (b) V-M(60), (c) V-M(240) and (d) Si-MMS.

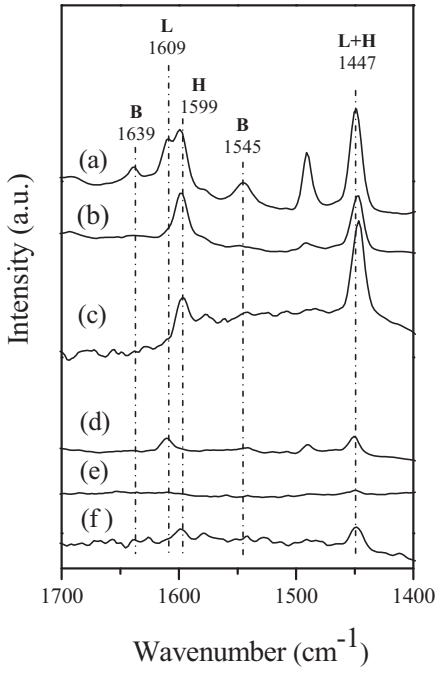

Fig. 4. FTIR spectra of pyridine adsorbed on the (a) V-M(20), (b) V-M(60), (c) V-M(240) after desorption at 100 °C and (d) V-M(20), (e) V-M(60), (f) V-M(240) after desorption at 200 °C.

framework of MCM-41 at the defect sites present in the mesoporous structure [22]. Therefore, this band can be interpreted, in our samples, in terms of the overlapping of both Si—OH groups and V—O—Si bonds vibrations. Anyway, when a metal is incorporated, the intensity of this band increases and this is generally considered to be a proof of the incorporation of the heteroatom into the framework [23,24].

Pyridine adsorption was followed by infrared spectroscopy to identify the number and nature of acid sites in V-M(x). Fig. 4 shows FT-IR spectra of the catalysts after pyridine adsorption and subsequent evacuation at 100 °C and 200 °C for all samples. In the spectra of V-M(x) a band at 1609 cm^{-1} overlapped to another at 1599 cm^{-1} in the case of smaller contents, appear and they are assigned to pyridine coordinately bound to Lewis sites and pyridine bonded to hydrogen, respectively [25–29]. All the samples show the band at 1447 cm^{-1} corresponding to pyridine bonded to both hydrogen and Lewis sites which frequently appears at 1450 cm^{-1} [25]. Moreover, the spectra show weak bands at 1545 and 1639 cm^{-1} which can be attributed to pyridine cations formed on Brønsted sites [29–31]. In addition, a band corresponding to vibration of pyridine associated with both, Lewis and Brønsted acid sites, was observed at 1490 cm^{-1}. One of the possible origins of the generation of Brønsted acid sites on the V-M(x) material could be the weakness of the strength of the SiO—H bonds due to the presence of $V^{\delta+}$ ions in the vicinity of the silanol groups existent in the structure [19]. When the smaller Si^{4+} ions are replaced by the $V^{\delta+}$ ion in the framework of the solid, the bond length of V—O—Si clearly differs from the one Si—O—Si which leads to some structure deformations.

Moreover, $V^{\delta+}$ ions in the vicinity of the hydroxyls carrying silicon could cause changes in the electron density around Si due to differences in electronegativity or to the local structure deformations resulting from the introduction of the vanadium into the framework, thus weakening the SiO—H bonds [26,32]. According to the analysis of chemisorption of pyridine followed by FT-IR, it can be concluded that the Lewis acid sites and the Brønsted acid sites evidenced in the V-M(x) catalysts increased proportionally according to the amount of V incorporated into the material. On the other hand, taking into account the relative intensity of the bands associated with the Lewis and Brønsted acid sites, after evacuation at 200 °C, the Lewis acidity resulted more important. Thus, the temperature programmed pyridine desorption reveals a relatively weak Brønsted acidity and medium Lewis sites on the V-M(x) which increases with V loading.

3.2. Catalytic activity

Since the UV-Vis-DR above characterization results showed V in the tetrahedral environmental in all catalysts with slight differences, it may be highly active in various oxidation reactions with peroxides as the oxidizing agent. Hence the synthesized catalysts were tested in the reaction of α-pinene oxidation with H_2O_2 at 70 °C. The products of α-pinene oxidation are shown in Scheme 1. The formation of product (1) is attributed to the oxidation of π bond, species (2) is formed by the rearrangement of (1), whereas species (3) and (4) are formed by hydrolysis and by the opening of oxirane ring. Products (5) and (6) are generated by oxidation of allylic C—H bond and finally, other products of over oxidation were all observed.

Before analyzing the results of the catalytic activity, we must consider the processes usually occurring in liquid-phase oxidation reactions with oxidants like H_2O_2 as oxygen donors. Usually H_2O_2 gets anchored on the active catalytic site, which may further react with the alkene to form the desired product. A parallel alternative reaction is the decomposition of H_2O_2 to water which can be favored by the presence of dimers or oligomers of metals. Furthermore, H_2O_2 can participate in the leaching reactions of the metal contained on the catalyst. Hence to maintain the preferential formation of oxidized products the oxidant concentration is kept as low as possible, thereby increasing the alkene reaction.

Fig. 5 shows the effect of the different V loadings in the final catalysts on the oxidation of α-pinene versus reaction time. As it can be seen, the conversion of α-pinene is in the range 10–13 mol %. The highest activity of the samples with lower V content (V-M(60) and V-M(240)) is thought to be due to the good dispersion of active sites, originated from isolated V species in a tetrahedral coordination located on the wall surface of the mesoporous channels [11]. Besides, the slight increase observed in the conversion when the V content of the samples is changed from 0.035 to 0.140 wt% could be related to the increase in the relative proportion of accessible tetrahedral V species located in the wall

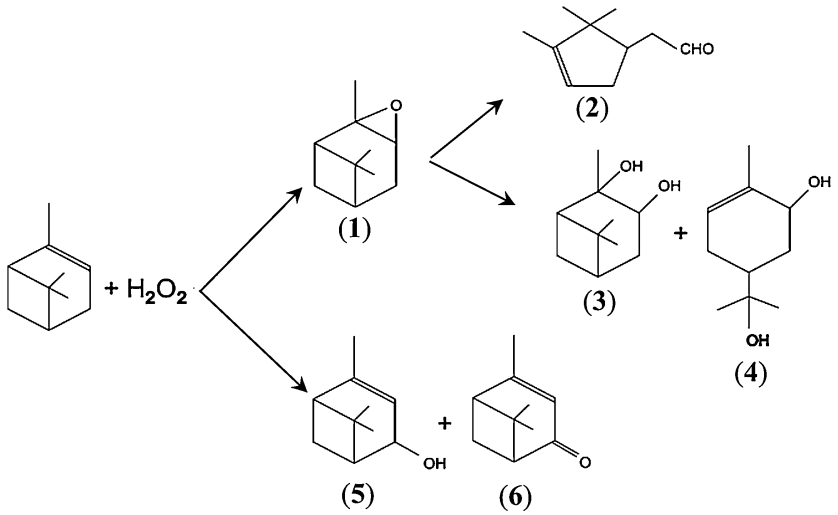

Scheme 1. Products obtained from α-pinene oxidation. α-Pinene oxide (**1**), campholenic aldehyde (2), 1,2 pinanediol (3), *trans*-sobrerol (4), verbenol (5), verbenone (6).

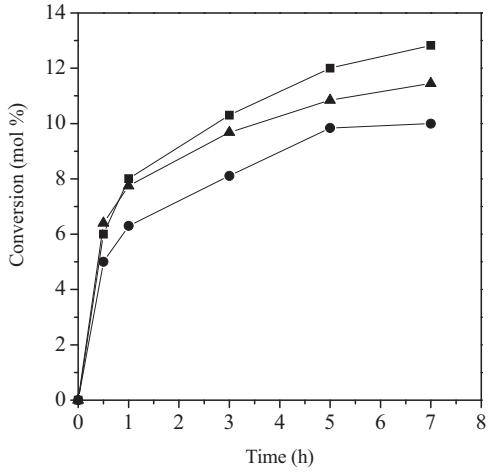

Fig. 5. Influence of the different Si/V molar ratios on the α-pinene conversion over V-M(*x*) versus reaction time under standards conditions (● Si/V: 20, ▲ Si/V: 240, ■ Si/V: 60).

surface (Table 1). Meanwhile, the reason for the lowest catalytic activity over the V-M(20) sample can be associated with the greatest percentage of extra-framework metal species, as oligonuclear $(V^{\delta+}\cdots O^{\delta-}\cdots V^{\delta+})_n$ nanoclusters (observed by UV-Vis-DR), compared with the V-M(240) and V-M(60).

In addition, blank experiments, without any catalyst or with V-free silica were carried out. The reaction did not proceed in the absence of the catalyst and the α-pinene conversion on pure silica Si-MMS was very low (<1 mol %). Hence the enhanced conversion observed over V-M(*x*) confirms the role of V ions in the present reaction.

The selectivity to the different products observed for all the synthesized catalysts in a 7 h reaction is shown in Table 2. Often, epoxidation and allylic oxidation are competitive processes in the oxidation of cyclic olefins and frequently both processes occur simultaneously giving a mixture of reaction products. Thus, allylic oxidation products were formed with high selectivity over V-M(240) being the verbenone the main reaction product.

It is also clear from Table 2 that the V-M(60) and V-M(20) catalysts exhibited high selectivity to campholenic aldehyde, 1,2 pinanediol, *trans*-sobrerol and over oxidation products. It is well known that in the isomerization of α-pinene oxide the distribution of products largely depends on the nature of surface sites [33–35]. In this regard, the isomerization of α-pinene oxide over Lewis acid sites leads to the formation of campholenic aldehyde (2), while Brønsted acid sites bring about the formation of 1,2 pinanediol (3) and *trans*-sobrerol (4) by hydrolysis and opening of oxirane ring and its rearranged hydrolysis product respectively [35,36]. The characterization data by FT-IR/Pyridine adsorption reported in the present work have confirmed that the number of both medium Lewis acid sites and weak Brønsted acid sites increases with V loading. Thus, the increase in the Brønsted acid sites and Lewis acid sites favors the formation of campholenic aldehyde, 1,2 pinanediol, *trans*-sobrerol and over oxidation products (Table 2). Probably, the presence of $(V^{\delta+}\cdots O^{\delta-}\cdots V^{\delta+})_n$ nanoclusters of increased size, mainly observed for the V-M(20) sample, is favoring the consecutive reactions of over-oxidation [37].

Another interesting result of the experiments is the increased conversion of the H_2O_2 on V-M(20) compared with the V-M(240) catalysts with the lowest vanadium content, while peroxide efficiency shows an opposite trend (Table 2). This behavior could be attributed to the above mentioned formation of extra-framework nanoclusters at high metal loadings which would be responsible for the consumption of peroxide and its decomposition to water. Thus, the decreased conversion of α-pinene may also account for the oligomerization of V species at the highest metal loading. Generally, octahedrally coordinated species are less active in oxidation reaction with peroxide because of the lack of free coordination sites. Thus, the low conversion for V-M(20) catalyst and its lowest peroxide efficiency indicate that the material contains dimeric-oligomeric V species. Besides, this material presents a smaller area than those with lower V content (Table 1). Probably, these nanoclusters species, placed both inside the channels and on the external surface [11], could diminish and block the accessibility to the active sites on the wall surface (isolated V ions) causing a further decrease of the catalytic activity [11].

On the other hand, according to literature, another measure of catalysts activity is the turnover number (TON), defined as moles converted per active site [38]. Thus, in the Fig. 6 there are presented TON values and the conversion of α-pinene for the different materials with respect to the metal molar loading, which is defined as moles of metal/100 g of catalyst. The TON values decrease strongly with increasing V content which would be indicating that much of the V incorporated is not effectively used for the catalytic oxidation.

At higher V content, the dispersion of V in the framework is low and polymeric V species become more abundant. Thus, more $(V^{\delta+}\cdots O^{\delta-}\cdots V^{\delta+})_n$ entities are formed, which are much less active toward oxidation reactions. In addition, the higher intrinsic activity

Table 2
α-Pinene oxidation with H_2O_2 on V-M(x) catalysts under standards conditions.

Sample	α-Pinene conversion(mol%)	H_2O_2		Selectivity[b](mol %)						
		Conversion (mol%)	Efficiency[a](mol%)	(1)	(2)	(3)	(4)	(5)	(6)	Over-oxidation products
V-M(20)	10.0	91.3	38.3	2.1	33.7	12.2	21.8	4.1	9.1	16.8
V-M(60)	12.8	84.5	53.2	4.7	13.4	15.9	36.3	11.4	7.8	10.5
V-M(240)	11.4	79.7	57.2	2.7	24.1	3.7	5.3	14.1	46.0	4.2

Standards conditions: α-pinene/H_2O_2 molar ratio = 4; catalyst = 9 gL^{-1}, temperature = 70 °C; solvent AcN, reaction time = 7 h.
[a] H_2O_2 efficiency: moles of products formed)/mol of H_2O_2 reacted.
[b] (1) α-Pinene oxide, (2) campholenic aldehyde, (3) 1,2 pinanediol, (4) *trans* sobrerol, (5) verbenol, (6) verbenone.

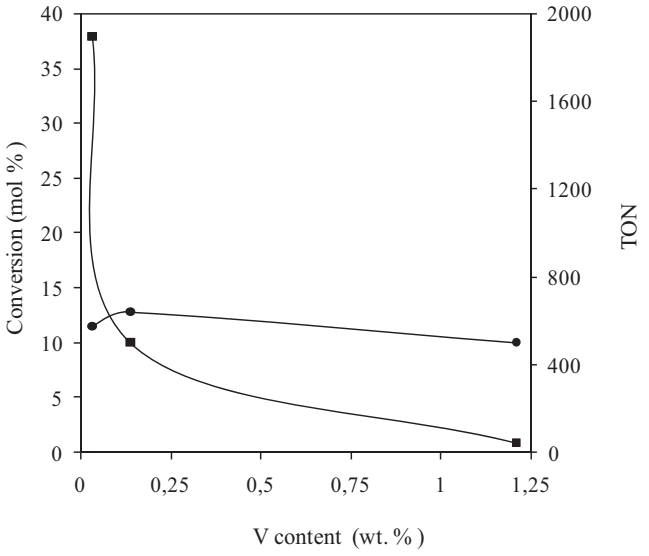

Fig. 6. Effect of V content in: α-pinene conversion (●) and TON (■).

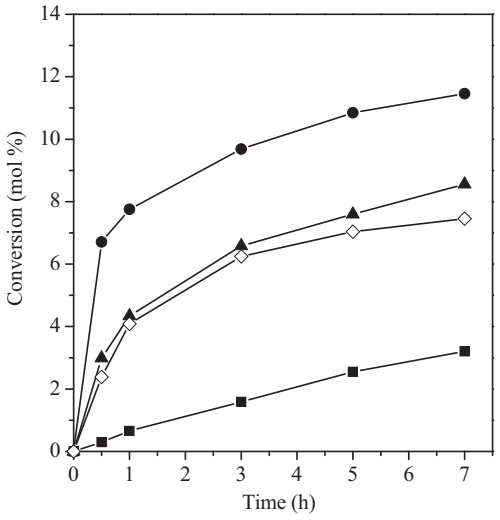

Fig. 7. Solvents effect on the conversion of α-pinene oxidation over V-M(240) catalyst, (● AcN, ▲ EtOH, ◊ *i*AOH, ■ MEK). Reaction conditions: α-pinene/H_2O_2 molar ratio: 4; solvent/α-pinene molar ratio: 15; temperature: 70 °C; reaction time: 7 h catalyst: 9 gL^{-1}.

Table 3
Characteristics of the solvents used in the oxidation of α-pinene on the V-M(240).

Solvent	EtOH	*i*AOH	AcN	MEK
Protic/aprotic	Protic	Protic	Aprotic	Aprotic
Boiling point (°C)	78.3	130.0	81.6	79.6
Dielectric constant	24.5	14.1	37.5	18.5
Dipolar moment (D)	1.69	1.69	3.92	2.72

for the catalyst with lower metal content would be giving account for the high dispersion and efficiency of the active sites incorporated on this material.

3.3. Solvents effect on the α-pinene oxidation

The choice of solvents for liquid-phase reactions is critical since factors such as the solubility of reagents, polarity, reactivity and acidity of the solvent, and the competitive chemisorption between solvent and reactants have a great influence on both the activity and selectivity of the solid catalyst [39–41]. In order to study the influence of the nature of the solvent on the α-pinene oxidation with H_2O_2, the V-M(240) material was selected taking into account its high turnover number and selectivity to verbenone. For this study, protic solvents: ethanol (EtOH) and isoamyl alcohol (*i*AOH) and aprotic solvents: acetonitrile (AcN) and methyl ethyl ketone (MEK) were selected. Table 3 shows the characteristics of the different solvents used and their protic/aprotic nature.

The solvent effect on the catalytic activity is presented in Fig. 7 which shows the evolutions of α-pinene conversion in each solvent as a function of reaction time. Among the solvents used, the best result was obtained with AcN, an aprotic solvent with elevated polarity and the highest dielectric constant. The order of reactivity observed was: AcN > EtOH > *i*AOH > MEK. The detected differences in activity could be related to the different interactions of the solvent molecules with the catalyst active centers.

Usually protic solvents take part in the elementary steps of the liquid-phase oxidation. Clerici and Ingallina [42] reported that the activity of titanium silicalites for oxidation of olefins is enhanced by the use of protic solvents (alcohols). They suggested that in the presence of ROOH and a coordinating solvent the reaction occurs with the formation of an active titanium hydroperoxo complex coordinated to the solvent forming a cyclic species. The species is formed prior to the approximation of the olefin to the metal–peroxo complex. In the case of AcN, which would not form the cyclic species, another possible explanation can be formulated. Taking into account the reaction mechanism for liquid phase oxidation with H_2O_2 on metal based catalysts which considers that solvent, H_2O_2 (in water) and H_2O can be adsorbed on the active site in a competitive way. Then, in aprotic solvents a cyclic species is formed in which water, instead of alcohol, is coordinated to metal centers and stabilizes the metal-peroxo complex trough a hydrogen bonding [43]. Indeed, taking into account that electron-donor capacity of water is lower than the alcohols (EtOH and *i*AOH), the intermediate constituted by water have a higher electrophilic character than the formed with the studied alcohols. Consequently, it shows a high intrinsic reactivity for the oxidation reaction. In addition, for aprotic solvents the activity increases with the polarity (AcN > MEK), which may be explained by the increase of the concentration of olefin in the vicinity of the active sites on hydrophilic surface. Besides, taking into account that AcN has more polarity, it would preferentially help to the formation of metal peroxo species [7]. On the order

Table 4
Influence of solvent on the selectivity during the oxidation of α-pinene on the V-M(240).

Solvent	Selectivity (mol%)						
	(1)	(2)	(3)	(4)	(5)	(6)	Other
AcN	2.7	24.1	3.7	5.3	14.1	45.6	4.2[a]
MEK	8.5	24.8	13.6	0.0	13.7	39.4	0.0
EtOH	0.8	15.0	1.1	1.3	2.9	42.3	38.3[b]
*i*AOH	0.1	14.0	1.4	1.6	4.0	43.6	35.3[b]

Reaction conditions: α-pinene/H_2O_2 molar ratio: 4; solvent/ α-pinene molar ratio: 15; temperature: 70 °C; reaction time: 7 h catalyst: 9 g L^{-1}.
(1) α-Pinene oxide, (2) campholenic aldehyde, (3) 1,2 pinanediol, (4) *trans*-sobrerol, (5) verbenol, (6) verbenone.
[a] Over oxidation products.
[b] Alkyl glycol ethers.

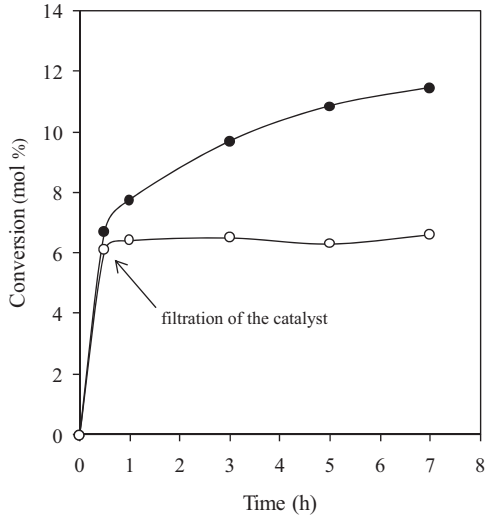

Fig. 8. Leaching experiment using V-M(240) in standard conditions with filtration of the catalyst at 0.5 h of reaction (○) and without filtration (●).

hand, the selectivity to products obtained after 7 h of reaction for each solvent is presented in Table 4.

As it can be seen when protic solvents were used, the selectivity to epoxide was very low, which could be due to opening of oxirane ring by the water and alcohol molecules forming the glycols and alkyl glycol ethers respectively.

3.4. Catalyst stability and recycling

The essential properties of solid catalysts are the stability of the active component with respect to leaching and the stability of the porous structure. The nature of the catalysis is also a crucial factor in the liquid-phase process. Since leaching of active metal species is a common phenomenon in mesoporous metallosilicates due to the destruction of the delicate solid pore wall surface under the reaction condition, stability/heterogenity studies are of primary importance for their further applicability. Since small amounts of leached metal species can have a significant effect on the entire catalytic activity, a rigorous proof of the heterogeneity of the catalyst is necessary. Usually, the leaching is promoted by the coordination ability of solvents on active metal sites and the use of aqueous oxidants. Hence in the present study we performed the following leaching studies on V-M(240). The catalyst was applied under the reaction conditions, and after thirty minutes it was removed by fast filtration; then the filtrate was applied under the reaction conditions. As shown in Fig. 8, the α-pinene conversion was not modified after the filtration of catalyst. This indicates that the oxidation process is truly heterogeneous and occurs on the catalyst

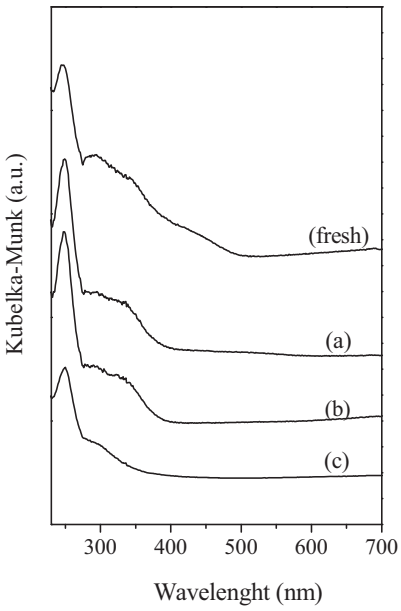

Fig. 9. Diffuse reflectance UV-Vis spectra of V-M(240) calcined in all cases, where: (a) after stirring for 2 h in the presence of acetonitrile/oxidant mixture, (b) after stirring for 2 h in the presence of solvent, (c) used after four catalytic cycles.

surface rather than in the solution. Even if very small amounts of V species are leached from the solid matrix during the oxidation process, the observed catalytic activity is not due to these species. Furthermore, ICP analysis data for the used V-M(240) only showed a low V leaching (6.9 % w/w) under the conditions used in this study.

In order to verify these results, two experiments have been carried out by modifying the reaction conditions: (a) The catalyst was stirred under reaction conditions in the presence of acetonitrile/oxidant mixture for two hours, the catalyst was removed by fast filtration and then the filtrate was applied under the reaction conditions with addition of substrate for five additional hours. (b) The catalyst was stirred in the presence of solvent for 2 h at 70 °C, the catalyst was removed by fast filtration and then the filtrate was applied under the reaction conditions with the addition of substrate and oxidant for five additional hours. In both cases no catalytic activity was observed. At the end of these experiments, the chemical analysis by ICP of V in solution for the both mother liquor ((a) and (b)) showed that 12.0 % and 6.6 % of the total V in the catalyst has leached into the solution as not active species. On the other hand, the results of conversion of hydrogen peroxide obtained in the experiment (a) are greater than those in (b) 83.2 and 10.0 % respectively at the end of reaction. This would indicate that the mechanism of leaching could be associated principally with the presence of hydrogen peroxide. Through the joint assessment of the stability tests and the values of leached V, it can be deduced that the presence of α-pinene in the reaction media prevents the leaching phenomena while the H_2O_2 promotes this leaching.

In addition, the V-M(240) samples used in the experiment (a) and (b) were analyzed by UV-Vis-DR and ICP-OES after calcination at 500° C for 12 h. UV-Vis-DR spectra are shown in Fig. 9. The band at ~ 260 nm adjudicated to isolated $V^{\delta+}$ cations in tetrahedral coordination with lattice oxygen on the walls surface of the mesoporous channels remains unchanged for all cases, which suggests that the isolated $V^{\delta+}$ cations are thermal and chemically stable. Meanwhile the band in the 300 nm region for the spectra, (a) and (b) is shifted to longer wavelengths and its intensity is decreased. The displacement can be attributed to the formation of larger aggregates caused by the further heat treatment [44]. Moreover, the reduction in the intensity of this band after the experiments (a) and (b) (Fig. 9, curves

Table 5
Catalytic performances of the recycled V-M(240) in the α-pinene oxidation with H_2O_2 under standards conditions.

Cycles	Time (h)	α-Pinene conversion (mol%)	Selectivity (mol%)						
			(1)	(2)	(3)	(4)	(5)	(6)	Other[b]
1	0.5	6.4	17.0	27.2	0.0	0.0	13.7	41.9	0.0
	7	11.4	2.7	24.1	3.7	5.3	14.1	45.9	4.2
1[a]	7	6.1	17.4	26.9	0.0	0.0	14.1	41.6	0.0
2	7	11.1	3.3	23.3	5.3	4.9	13.4	49.9	0.0
3	7	11.2	8.9	21.5	5.7	3.8	10.0	50.2	0.0
4	7	10.0	10.7	21.9	4.9	2.7	8.7	51.1	0.0

[a] After filtration of catalyst.
[b] Over oxidation products.

Table 6
Conversion/efficiency of H_2O_2 and analysis by ICP of V in solution for several catalytic cycles.

Cycles	Conversion H_2O_2 (mol%)	Efficiency H_2O_2 (mol%)	Lost V detected in solution (%)[a]
1	79.7	57.2	7.1
2	67.9	65.4	2.9
3	22.8	98.0	n.d
4	22.5	100.0	n.d

[a] At the end of the reaction.

(a) and (b)) indicates the decrease of the amount of the extra-framework nano-clusters. These results show that the solvent and H_2O_2 are involved in the lixiviation reaction forming inactive soluble V species, while the isolated $V^{\delta+}$ cations are stable active sites for the oxidation of α-pinene.

An important issue that must be addressed while studying liquid-phase oxidation over a solid catalyst is the possibility of catalyst recycling. Thus, the stability of V-M(240) was investigated by recycle experiment. At the end of reaction, the catalyst was recovered from the reaction solution by filtration. After regeneration at 500 °C overnight, the catalyst was reused for several catalytic cycles. We found that the V-M(240) catalyst maintained its activity and selectivity for at least four catalytic cycles, Table 5. In addition we calculate the initial rates for these experiments and the found values were 10.52, 9.92, 9.89 and 10.21 (mmol/g. h) for the first, second, third and fourth catalytic cycle respectively. These results confirm that the catalyst conserved its catalytic activity for at least four cycles.

It is worth noting that while the H_2O_2 efficiency increases with the catalytic cycles number, the vanadium leaching decreases (Table 6). This behavior could be correlated with the above mentioned interaction of the extraframework nano-clusters with the solvent and oxidant. As H_2O_2 participates in the leaching reactions, less H_2O_2 is available for the oxidation reaction and therefore the efficiency is low.

It was surprising to find that no vanadium leached after the second catalytic cycle. This result is in agreement with the result obtained by UV-Vis-DR spectroscopy (Fig. 9 (c)) where extra-framework nanoclusters practically disappeared in the used material after four catalytic cycles.

Finally, no significant changes in the structure, evidenced by XRD (not shown), were observed by this catalyst after four catalytic cycles. The N_2 adsorption measurements revealed a 7.08 % increase in the specific surface, which can probably be explained by the decrease of the amount of extra-framework nano-cluster already observed by UV-Vis-DR. These experiences indicate that V-M(240) has a good long-term stability and activity.

4. Conclusions

In this study physicochemical properties of V containing molecular sieves V-M(x) were investigated by different techniques. The UV–Vis-DR spectra confirm the existence of two different types of $V^{\delta+}$ species. It is possible to suggest that V is incorporated into two different framework sites, one inside the wall and the other on the wall surface of the channels of MCM-41 structure. Moreover, the presence of oligonuclear $(V^{\delta+}\cdots O^{\delta-}\cdots V^{\delta+})_n$ nano-clusters, arising from an incipient oligomerization of V species could also be identified. FT-IR and Raman spectra provided strong evidences that most the vanadium species were incorporated into the framework as isolated species or, at least, highly dispersed on the surface.

The catalytic activity of V-M(x) was tested for the oxidation of α-pinene with H_2O_2. The main reaction products were verbenone, *trans*-sobrerol and campholenic aldehyde. It was shown that the conversion of α-pinene and the distribution of products depend on the V content in V-M(x) materials. The higher turnover numbers of the catalyst with lower metal content (1889) would be giving account for the high dispersion and efficiency of the isolated V sites incorporated on the wall surface of the channels of MCM-41 structure. Meanwhile, the lowest catalytic activity over the sample with the highest V content can be associated with the greatest percentage of V extra-framework which would be responsible for the consumption of peroxide and its decomposition to water, resulting in lower H_2O_2 efficiency and α-pinene conversion.

The characterization data by FT-IR/Pyridine adsorption have confirmed that the number of both medium Lewis acid sites and weak Brønsted acid sites increases with V loading. Thus, the increase in the Brønsted acid sites and Lewis acid sites favors the formation of campholenic aldehyde, 1,2 pinanediol, *trans*-sobrerol and over oxidation products. The use of several solvents showed that the highest α-pinene conversions were obtained in the following order: AcN > EtOH > *i*AOH > MEK. The higher activity and selectivity to verbenone obtained with AcN, an aprotic solvent with elevated polarity and the highest dielectric constant can be explained by the increase of the concentration of olefin in the vicinity of the active sites on hydrophilic surface. Using aprotic solvents, the catalytic activity was increased and the formation of alkyl glycol ethers as by-product was not observed.

Leaching experiments demonstrated that very small amounts of V species were leached from the solid matrix during the first and second cycle catalytic (7.1 and 2.9 % w/w of the total V in the catalyst, respectively). AcN and H_2O_2 are involved in the lixiviation reaction forming inactive soluble V species, while the isolated $V^{\delta+}$ cations are stable active sites for the oxidation of α-pinene. Recycling studies and the characterization of the used catalyst indicate that the material is structurally stable and it can be used repeatedly without activity and selectivity loss during several cycles.

Acknowledgments

The authors would like to thank CONICET and UTN-FRC for their financial support and scholarships, also to the Laboratorio de Nanoscopía y Nanofotónica, INFIQC-CONICET/UNC, Sistema Nacional de Microscopía – MINCyT for the Raman facilities. The

authors also thank to Geol. J. Fernandez for FT-IR, to N. Waisman, M. Ponte, M. Romero for their experimental contribution and M. Martinez for the linguistic contributions.

References

[1] P.A. Robles-Dutenhefner, B.N.S. Brandaob, L.F. de Sousaa, E.V. Gusevskaya, Appl. Catal. A 399 (2011) 172–178.
[2] J. Trissa, S.B. Halligudi, J. Mol. Catal. A: Chem. 229 (2005) 241–247.
[3] Z. Luan, J. Xu, H. He, J. Klinowski, L. Kevan, J. Phys. Chem. 100 (1996) 19595–19602.
[4] Q.H. Zhang, W. Yang, X.X. Wang, Y. Wang, T. Shishido, K. Takehira, Micropor. Mesopor. Mat. 77 (2005) 223–234.
[5] Y.M. Liu, S.H. Xie, Y. Cao, H.Y. He, K.N. Fan, J. Phys. Chem. C 114 (2010) 5941–5946.
[6] G.A. Du, S.Y. Lim, Y.H. Yang, C. Wang, L. Pfefferle, G.L. Haller, Appl. Catal. A 302 (2006) 48–61.
[7] S. Shylesh, A.P. Singh, J. Catal. 228 (2004) 333–346.
[8] K. Wu, B. Li, C. Han, J. Liu, Appl. Catal. A 479 (2014) 70–75.
[9] S. Shylesh, A.P. Singh, J. Catal. 233 (2005) 359–371.
[10] P. Selvam, S.E. Dapurkar, J. Catal 229 (2005) 64–71.
[11] C. Chanquía, A. Cánepa, K. Sapag, P. Reyes, E. Herrero, S. Casuscelli, G. Eimer, Top. Catal. 54 (2011) 160–169.
[12] K.J. Chao, C.N. Wu, H. Chang, J. Phys. Chem. B. 101 (1997) 6341–6349.
[13] I.W.C.E. Arends, R.A. Sheldon, Top. Catal. 19 (2002) 133–141.
[14] C.M. Chanquía, A.L. Cánepa, J. Bazán-Aguirre, K. Sapag, E. Rodríguez-Castellón, P. Reyes, E.R. Herrero, S.G. Casuscelli, G.A. Eimer, Micropor. Mesopor. Mater. 151 (2012) 2–12.
[15] C.W. Lee, W.J. Lee, Y.K. Park, S. Park, Catal. Today 61 (2000) 137–141.
[16] T. Sen, V. Ramaswamy, S. Ganaphaty, P. Rajamohanan, S. Sivasanker, J. Phys. Chem. 100 (1996) 3809–3817.
[17] B. Solsona, T. Blasco, J.M. López, M.L. Peña, F. Rey, A. Vidal-Moya, J. Catal. 203 (2001) 443–452.
[18] M. Peña, A. Dejoz, V. Fornés, F. Rey, M. Vázquez, J. López Nieto, Appl. Catal. A 209 (2001) 155–164.
[19] G. Eimer, S. Casuscelli, G. Ghione, M. Crivello, E. Herrero, Appl. Catal. A: Gen. 298 (2006) 232–242.
[20] E. Vaschetto, G. Monti, E. Herrero, S. Casuscelli, G. Eimer, Appl. Catal. A 453 (2013) 391–402.
[21] C.H. Lee, T.S. Lin, C.Y. Mou, J. Phys. Chem. B 107 (2003) 2543–2551.
[22] A. Corma, Chem. Rev. 97 (1997) 2373–2419.
[23] F. Farzaneh, E. Zamanifar, C. Williams, J. Mol. Catal. A: Chem. 218 (2004) 203–209.
[24] B. Reddy, I. Ganesh, B. Chowdary, Catal. Today 49 (1999) 115–121.
[25] A. Sakthivel, S. Dapurkar, N. Gupta, S. Kulshreshtha, P. Selvam, Micropor. Mesopor. Mater. 65 (2003) 177–187.
[26] D. Trong On, S. Nguyen, V. Hulea, E. Dumitriu, S. Kaliaguine, Micropor. Mesopor. Mater. 57 (2003) 169–180.
[27] D. Srinivas, R. Srivastava, P. Ratnasamy, Catal. Today 96 (2004) 127–133.
[28] T. Conesa, J. Hidalgo, R. Luque, J. Campelo, A. Romero, Appl. Catal. A 299 (2006) 224–234.
[29] C. Otero Areán, M. Rodríguez Delgado, V. Montouillout, J. Lavalley, C. Fernández, J. Cuart Pascual, J. Parra, Micropor. Mesopor. Mater. 67 (2004) 259–269.
[30] L. Chen, L. Noreña, J. Navarrete, J. Wang, Mater. Chem. Phys. 97 (2006) 236–242.
[31] H. Kosslick, G. Lischke, G. Walther, W. Storek, A. Martin, R. Fricke, Micropor. Mater. 9 (1997) 13–33.
[32] J. Anderson, C. Fergusson, I. Rodriguez-Ramos, A. Guerrero-Ruiz, J. Catal. 192 (2000) 344–354.
[33] G. Neri, G. Rizzo, C. Crisafulli, L. De Luca, A. Donato, M.G. Musolino, R. Pietropaolo, Appl. Catal. A 295 (2005) 116–125.
[34] W.F. Holderich, J. Roseler, G. Heitmann, A.T. Liebens, Catal. Today 37 (1997) 353–354.
[35] Y.W. Suh, N.K. Kim, W.S. Ahn, H.K. Rhee, Mol. Catal. A: Chem. 198 (2003) 309–316.
[36] Y.W. Suh, N.K. Kim, W.S. Ahn, H.K. Rhee, J. Mol. Catal. A: Chem. 174 (2001) 249.
[37] Y.M. Liu, Y. Cao, N. Yi, W.L. Feng, W.L. Dai, S.R. Yan, H.Y. He, K.N. Fan, J. Catal. 224 (2004) 417–428.
[38] J.M. Thomas, W.J. Thomas, Principles of Heterogeneous Catalysis, VCH, New York, 1997.
[39] L. Gilbert, C. Mercier, Stud. Surf. Sci. Catal. 78 (1993) 51–66.
[40] J. Van der Waal, H. van Bekkum, J. Mol. Catal. A: Chem. 124 (1997) 137–146.
[41] T. Tatsumi, M. Nakamura, S. Nigishi, H. Tominaga, J. Chem. Soc. Chem. Commun. (1990) 476–477.
[42] M.G. Clerici, P. Ingallina, J. Catal. 140 (1993) 71–83.
[43] A. Corma, P. Esteve, A. Martinez, J. Catal. 161 (1996) 11–19.
[44] D. Beydoun, R. Amal, G. Low, S. McEvoy, J. Nanopart. Res. 1 (1999) 439–458.